Chinese Journal of Polymer Science Vol. 35, No. 1, (2017), 87–97

Chinese Journal of Polymer Science

A Robust and Soluble Nanopolymer Based on Molecular Grid-based Nanomonomer*

Quan-you Feng[a†], Ye-long Han[a†], Meng-na Yu[a], Bin Li[a], Ying Wei[a], Ling-hai Xie[a**] and Wei Huang[a, b**]

[a] *Center for Molecular Systems and Organic Devices (CMSOD), Key Laboratory for Organic Electronics and Information Displays & Institute of Advanced Materials (IAM), Jiangsu National Synergetic Innovation Center for Advanced Materials (SICAM), Nanjing University of Posts & Telecommunications, Nanjing 210023, China*

[b] *Key Laboratory of Flexible Electronics (KLOFE) & Institute of Advanced Materials (IAM), Jiangsu National Synergetic Innovation Center for Advanced Materials (SICAM), Nanjing Tech University (NanjingTech), Nanjing 211816, China*

Abstract Shape persistent conformations reduce the complexity of polymer materials. Herein, we propose a concept on the nanopolymer that is a nanoscale polymer chain with the repeat units of nanomonomers. In this article, a soluble organic nanopolymer of wide bandgap semiconductors was synthesized by the Yamamoto polymerization of nanogrid monomer as the repeat units with the rectangle size of ~1.7 nm × 1.2 nm. The alkyl side chain substituent at 9-position of fluorenes guarantees the polygrid with excellent solubility. Tetrafluorenes in the conjugation-interrupted backbones of polygrid acts as the active light-emitting centers without obvious green band in the fluorescence spectra of the films after 10 h annealing at 180 °C, indicating this nanopolymer exhibits excellent spectral stability. Such soluble nanopolymers will be the fifth-generation of macromolecular materials with a potential character of overall performance improvement.

Keywords Conformation; Polyfluorenes; Polygirds; Nanopolymers; Nanomaterials; Stability

Electronic Supplementary Material Supplementary material is available in the online version of this article at http://dx.doi.org/10.1007/s10118-016-1856-7.

INTRODUCTION

Wide bandgap polymers are the key components in the field of the future electronics for information and energy industries[1, 2]. However, the organic wide bandgap polymers are not superior to the inorganic counterparts such

* This work was partially financially supported by the National Natural Science Funds for Excellent Young Scholar (No. 21322402), the National Natural Science Foundation of China (Nos. 21274064, 21504041, 21504047 and 61136003), Excellent Science and Technology Innovation Team of Jiangsu Higher Education Institutions (2013), Synergetic Innovation Center for Organic Electronics and Information Displays, the Natural Science Foundation of Jiangsu Province (Nos. BK20150834 and BM2012010) and Open Project from State Key Laboratory of Supramolecular Structure and Materials at Jilin University (No. klssm201612). Project funded by the Priority Academic Program Development of Jiangsu Higher Education Institutions (PAPD) and Nanjing University of Posts and Telecommunications Scientific Foundation (NUPTSF) (No. NY214179).

** Corresponding authors: Ling-hai Xie (解令海), E-mail: iamlhxie@njupt.edu.cn
Wei Huang (黄维), E-mail: iamwhuang@njupt.edu.cn

† These authors contributed to this work equally.

Received May 16, 2016; Revised June 22, 2016; Accepted June 23, 2016
doi: 10.1007/s10118-016-1856-7

as GaN, ZnO, SiC and diamonds, although they have the advantages, such as the low-cost wetting procedures, the mechanical flexibility, the large area and the batch production[3–6]. Up to update, the molecular design is still the crucial way to improve the device parameters, such as the efficiency of polymer light emitting diodes (PLED) and solar cells, the mobility in the field effect transistor (FET), the stability and reliability as well as the repeatable procedures[7–10]. In order to efficiently improve the performance, the prerequisite is to clarify the defect mechanisms[11–14]. Concretely, the typical defect types include the chemical species defects that were induced by thermal, electrical/voltage, photo-irradiation; conformation defects with twist or bending, even deformation and entanglements; and the molecular packing defects by the aggregates or the field-induced aggregation. Recently, the third possible mechanism is ascribed to the conformation bending that can induce green-band (g-band) defects in polyfluorenes[15], while the rigid conformation makes them stable by virtue of the formation of β-phase[14]. Hence, the conformation polymorphisms are one of the most important factors to change the charge and excitons[16]. As a result, the complexity of the conjugated polymers not only deteriorates the stability by *in situ* generation of conformational defects[14, 17, 18], but also makes the control procedures difficult owing to the supramolecular sensitivity to the external conditions, which is the major origin to handle the improvement in plastic electronics.

In the past decades, many efforts have been paid to control the molecular structures for the improvement of device performances. For example, there are several demonstrated chemical approaches, such as the alkyl side chain engineering[19–23], the supramolecular approaches *via* polyrotaxane[24–26], the external conditions *via* mesoscale methods[17], as well as the combinational strategies. However, most of them are limited for the effectiveness, efficiency and extensibility. Nevertheless, it is of great significance to explore the unprecedented molecular design to fully improve overall performances for the next-generation polymer semiconductors. Nanostructures facilitate the polymer chains shape persistent by virtue of the robust conformation to avoid the defects. We define the nanopolymer as one kind of new-concept polymers that consist of the repeat units of nanomonomers linked by the covalent bonds. The nanopolymers with rigid nanoscale backbones may exhibit higher quantum yields and morphology stability by means of constricted conformation motion that would be a crucial factor to promote commercialization of plastic electronic devices[27–32]. Furthermore, the shape-persistent nanopolymers would integrate the advantages of not only conjugated polymers that are processable owing to the good solubility, but also the one-dimensional carbon nanotube (CNT) that exhibit excellent mechanical strength with the potential applications of the flexible and wearable e-textile devices. In addition, the covalent nanopolymers may provide a diverse molecular platform to explore the multifunctional molecular engineering for the smart materials with hierarchical coupling interaction of functions.

The soluble nanopolymers can be easily fabricated by the combination of organic reaction with polymerization. Compared to the macrocycles, the molecular grids with well-defined linkage sites offer the rectangular supermonomernodes that facilitate the generation of polymers, frameworks and networks. Previously, we get insight into the bulky diarylfluorenes with shape-persistent vertical linkage that allows for creating a kind of porous polymers. Herein, we report the use of nanogrids as the nanomonomers to fabricate the first nanopolymer serving as new-generation wide bandgap polymer semiconductors. As demonstrated in Scheme 1, we show a fluorene-based polygrid as a model of soluble one-dimensional nanopolymer. This polygrid also consists of a rectangular-shape monomer with a size of ~1.7 nm × 1.2 nm. In our design, the 9-substituent groups at fluorenes provide the alkyl and alkoxy side chains that guarantee the solubility after the polymerization. The rectangular grid nanomonomer is obtained by the molecular installing technology (MIT)[33] of L-based route *via* the final step of fluorenol's welding and joining protocol[34–37]. The chemical structures and physicochemical parameters of the obtained polymers are characterized by nuclear magnetic resonance (NMR), matrix-assisted laser desorption/ionization–time-of-flight mass spectrometry (MALDI-TOF-MS), gel permeation chromatography (GPC), thermogravimetric analysis (TGA) and differential scanning calorimetry (DSC) as well as UV-Visible absorption spectroscopy and fluorescence spectroscopy (UV/PL). The nanopolymer chains provide a chance to update polymer science and technology with extensive applications.

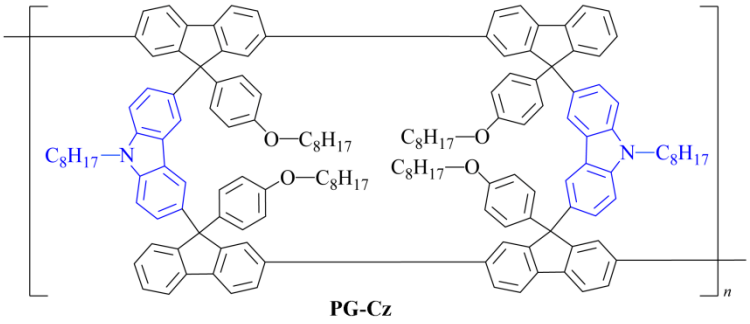

PG-Cz

Scheme 1 Chemical structure of the fluorene-based nanopolymer

EXPERIMENTAL

Materials

All reagents were purchased from Sigma-Aldrich, Merck and Alfa Aesar, and used as received unless stated otherwise. Anhydrous tetrahydrofuran (THF) (HPLC grade) was collected from solvent purification systems. Anhydrous chloroform was pre-dried over molecular sieves. 2,7-Dibromo-9-(4-(octyloxy)phenyl)-9H-fluoren-9-ol (**a**)[37] and 9-(4-(octyloxy)phenyl)-2-(4,4,5,5-tetramethyl-1,3,2-dioxaborolan-2-yl)-9H-fluoren-9-ol (**2**)[34] were synthesized according to our reported method.

Characterizations

^{1}H- and ^{13}C-NMR were recorded on a Bruker 400 MHz spectrometer in $CDCl_3$ with tetramethylsilane (TMS) as the interval standard. Mass spectra were recorded on a Shimadzu GCMS 2010 PLUS. For the MALDI-TOF MS analysis, the spectra were recorded in the reflective mode, and the substrates were used. GPC analysis was performed on a HP1100 HPLC system equipped with the 7911GP-502 and GP NXC columns using polystyrenes as the standard and THF as the eluent at a flow rate of 1.0 mL/min at 25 °C. DSC measurement was acquired using a Shimadzu Instruments DSC-60A. DSC data were collected from 30 °C to 245 °C at a rate of 10 K/min for both of the baseline and the samples. TGA were conducted by a Shimadzu DTG-60H under a heating rate of 10 K/min and a nitrogen flow rate of 50 cm^3/min. Cyclic voltammetric (CV) studies were conducted using an CHI660C Electrochemical Workstation in a typical three-electrode cell with a platinum sheet working electrode, a platinum wire counter electrode, and a silver/silver nitrate (Ag/Ag^+) reference electrode. All electrochemical experiments were carried out under a nitrogen atmosphere at room temperature in an electrolyte solution of 0.1 mol/L tetrabutylammoniumhexafluorophosphate (n-Bu_4NPF_6) in CH_3CN at a sweeping rate of 0.1 V/s.

Preparation of Polymer Grids Films for Optical Analysis

The quartz cells of 10 mm thickness were used to measure the spectra of the solutions. The pristine films of PODPF were spin-coated on the quartz substrates from the toluene solution (10 mg/mL) using KW-4A (from the Institute of Micro-Electronics of Chinese Academy of Science) at 1500 r/min for 30 s. The annealing films were prepared by spin-coated from toluene solutions (concentration: 10 mg/mL) onto the quartz plates and then thermally annealed in air at 180 °C for 0, 2, 5 and 10 h. Absorption spectra were measured with a Shimadzu UV-3600 spectrometer at 25 °C, and the emission spectra were recorded on a Shimadzu RF-5301(PC) luminescence spectrometer. The quartz cells of 10 mm thickness were used to measure the spectra of the solutions. The reported absorbance of the samples has been corrected for the solvent background. The excitation wavelength was 360 nm. To measure the fluorescence lifetime, the incident 390 nm, 150 fs laser pulses were generated from a Coherent TOPAS-C optical parametric amplifier; pumped by a 1 kHz Coherent Legend regenerative amplifier that is seeded by a Coherent Vitesse oscillator. These input laser pulses were focused by a lens (f = 20 cm) on the samples' solution in a 1 mm thick quartz cell (beam spot ~1 mm inside the cell). The emission from the samples was collected at a backscattering angle of 150° by a pair of lenses and directed to an Optronis Optoscope TM streak camera system which has an ultimate temporal resolution of 6 ps.

Polymer Synthesis

*3-(2,7-Dibromo-9-(4-(octyloxy)phenyl)-9H-fluoren-9-yl)-9-octyl-9H-carbazole (**1**) synthesis*

A solution of boron trifluoride-diethyl ether complex (7.80 g, 6.96 mL) in 5 mL of dichloromethane (DCM) was added dropwise to a solution of compound **a** (10 g, 18.37 mmol) and *N*-octylcarbazole (51.33 g, 183.70 mmol) in DCM (95 mL). The reaction mixture was stirred at room temperature (r.t., 25 °C) for 24 h. Ethanol (50 mL) and water (50 mL) was successively added to quench the reaction. And then the mixture was separated and the aqueous phase was extracted with DCM. The combined DCM layers were washed and dried ($MgSO_4$). After removal of the solvent, the remaining crude product was purified by the column chromatography using an eluent of petroleum ether (PE):DCM = 20:1 (*V*:*V*) to provide a white solid compound **1** (14.10 g, 97%). MALDI-TOF-MS (*m*/*z*) for $C_{47}H_{51}Br_2NO$, Calcd.: 805.2 [M^+]; Found: 805.2. ^{1}H-NMR (400 MHz, $CDCl_3$, δ): 7.96 (d, J = 7.6 Hz, 1H), 7.84 (s, 1H), 7.61 (d, J = 8.0 Hz, 2H), 7.55 (d, J = 1.6 Hz, 2H), 7.48 (dd, J_1 = 8.0 Hz, J_2 = 1.6 Hz, 2H), 7.43 (m, 1H), 7.37 (d, J = 8.0 Hz, 1H), 7.27 (m, 1H), 7.21 (dd, J_1 = 8.6 Hz, J_2 = 1.8 Hz, 1H), 7.17 (d, J = 8.0 Hz, 1H), 7.13 (d, J = 6.8 Hz, 2H), 6.79 (d, J = 6.8 Hz, 2H), 4.24 (t, J = 7.2 Hz, 2H), 3.93 (t, J = 6.4 Hz, 2H), 1.73–1.88 (m, 4H), 1.26–1.41 (m, 20H), 0.84–0.90 (m, 6H). ^{13}C-NMR (101 MHz, $CDCl_3$, δ): 158.49, 154.48, 140.99, 139.67, 138.10, 137.03, 135.10, 130.90, 129.69, 129.35, 126.08, 125.97, 122.77, 122.77, 122.07, 121.76, 120.64, 119.72, 119.00, 114.57, 108.92, 68.08, 65.40, 43.23, 32.05, 32.00, 29.58, 29.56, 29.48, 29.36, 29.19, 27.48, 26.30, 22.91, 22.83, 14.39, 14.35.

*7'-Bromo-9'-(9-octyl-9H-carbazol-3-yl)-9,9'-bis(4-(octyloxy)phenyl)-9H,9'H-[2,2'-bifluoren]-9-ol (**3**) synthesis*

In a three-necked schlenk flask (150 mL), compound **1** (11.80 g, 14.64 mmol), compound **2** (2.50 g, 4.88 mmol), tetra(triphenylphosphine) palladium(0) (340 mg, 0.29 mmol) were added. The flask was evacuated and back-filled with nitrogen atmosphere over three times, after which degassed toluene (40 mL), THF (40 mL) and K_2CO_3 aqueous solution (2 mol/L, 20 mL) were injected into the flask through a syringe. The mixture was heated up to 85 °C and stirred for 48 h. Water (100 mL) was successively added to quench the reaction. And then the mixture was separated and the aqueous phase was extracted with DCM. The combined DCM layers were washed and dried ($MgSO_4$). After removal of the solvent, the remaining crude product was purified by the column chromatography using PE:DCM:ethyl acetate (EA) = 16:1:1 (*V*:*V*:*V*) as the eluent to provide a yellow solid compound **3** (5.0 g, 86%). MALDI-TOF-MS (*m*/*z*) for $C_{74}H_{80}BrNO_3$, Calcd.: 1109.5 [M^+]; Found: 1109.1. ^{1}H-NMR (400 MHz, $CDCl_3$, δ): 7.91–7.96 (m, 2H), 7.77 (d, J = 8.0 Hz, 1H), 7.62–7.65 (m, 4H), 7.55–7.57 (m, 2H), 7.47–7.53 (m, 3H), 7.13–7.45 (m, 12H), 6.72–6.81 (m, 4H), 4.24 (m, 2H), 3.85–3.94 (m, 4H), 2.46 (s, 1H), 1.70–1.90 (m, 6H), 1.25–1.44 (m, 30H), 0.84–0.91 (m, 9H). ^{13}C-NMR (101 MHz, $CDCl_3$, δ): 158.47, 158.26, 158.12, 154.81, 154.76, 154.26, 152.94, 151.22, 150.86, 150.81, 141.60, 140.91, 140.82, 139.49, 139.43, 139.14, 139.08, 138.64. 138.25, 137.94, 137.54, 136.85, 135.55, 134.87, 134.81, 130.72, 130.58, 129.50, 129.28, 129.16, 129.08, 128.40, 128.24, 128.16, 126.16, 126.60, 126.09, 126.03, 125.89, 125.76, 125.64, 124.77, 122.70, 122.58, 121.82, 121.57, 121.40, 120.48, 120.34, 120.12, 119.64, 119.52, 118.75, 118.66, 114.34, 114.31, 114.20, 108.72, 108.62, 83.45, 67.92, 65.16, 43.19, 31.83, 29.73, 29.38, 29.26, 29.18, 29.03, 27.33, 26.10, 22.67, 22.62, 14.12.

*Monomer of polymer grid incorporating N-octylcarbazole units (**NGM-Cz**) synthesis*

To a solution of boron trifluoride-diethyl ether complex (6.36 g, 5.68 mL) in DCM (500 mL) was added dropwise a solution of compound **3** (2.50 g, 2.25 mmol) in DCM (200 mL). The reaction mixture was stirred at r.t. (25 °C) for 24 h. Ethanol (50 mL) and water (50 mL) was successively added to quench the reaction. Then the mixture was separated and the aqueous phase was extracted with DCM. The combined DCM layers were washed and dried ($MgSO_4$). After removal of the solvent, the remaining crude product was purified by the column chromatography using PE:DCM = 8:1 (*V*:*V*) as the eluent to provide a white solid compound **NGM-Cz** (1.18 g, 24%). MALDI-TOF-MS (*m*/*z*) for $C_{148}H_{156}Br_2N_2O_4$, Calcd.: 2186.0 [M^+]; Found: 2185.7. ^{1}H-NMR (400 MHz, $CDCl_3$, δ): 6.69–8.17 (m, 54H), 3.94–4.17 (m, 12H), 1.79 (br, 12H), 1.35 (br, 60H), 0.94 (br, 18H).

^{13}C-NMR (101 MHz, $CDCl_3$, δ): 158.39, 158.30, 158.15, 158.08, 157.74, 155.06, 155.00, 154.01, 153.13, 153.00, 152.76, 152.23, 152.12, 152.06, 151.76, 141.84, 141.78, 141.43, 141.09, 140.19, 140.12, 139.90, 139.73, 139.63, 139.38, 139.31, 139.11, 139.02, 138.87, 138.41, 138.11, 138.03, 137.93, 137.65, 136.29, 136.10, 136.00, 135.87, 135.76, 134.49, 132.27, 130.82, 130.63, 129.81, 129.50, 129.23, 128.35, 127.70, 127.34, 127.18, 126.99, 126.59, 126.47, 126.05, 125.80, 125.64, 124.90, 123.65, 122.52, 122.41, 122.24, 121.60, 121.49, 121.45, 121.23, 121.13, 120.96, 120.68, 120.41, 120.05, 118.95, 118.40, 116.37, 114.55, 114.29, 114.15, 108.75, 108.52, 107.99, 67.99, 65.38, 65.15, 65.06, 65.00, 64.86, 43.24, 34.33, 32.05, 31.96, 31.93, 31.91, 31.88, 31.86, 31.56, 30.44, 30.33, 29.99, 29.83, 29.79, 29.64, 29.52, 29.50, 29.48, 29.44, 29.40, 29.36, 29.33, 29.23, 29.17, 29.05, 27.32, 26.62, 26.38, 26.25, 26.23, 26.17, 26.10, 22.80, 22.77, 22.71, 21.33, 14.25, 14.22, 14.19.

*Polymer grid incorporating N-octylcarbazole units (**PG-Cz**) synthesis*

647 mg (0.30 mmol) of **NGM-Cz** was added to the DMF (5 mL) and toluene (5 mL) solution containing $Ni(COD)_2$ 195 mg (0.71 mmol), 1,5-cyclooctadiene 0.09 mL (0.71 mmol), and bipyridyl 111 mg (0.71 mmol) in a 50 mL Schlenk tube under argon. The reaction mixture was stirred for 36 h at 90 °C to obtain a dark blue solution. The bromobenzene was added to the solution for terminating the reaction. After the mixture was cooled to room temperature, 10 mL of THF and 1.0 mL of hytrazine hydrate were added for quenching the activator. The precipitate was separated by filtration. The solution was further purified by subjecting to the alumina (Al_2O_3) column chromatography eluted with THF to afford **PG-Cz** as a white powder (556 mg, 86%). GPC: M_n = 1.04 × 10^4, M_w = 1.70 × 10^4, PDI = 1.63. ^{1}H-NMR (400 MHz, $CDCl_3$, δ): 6.57–7.63 (m, 54H), 3.87 (br, 12H), 1.71 (br, 12H), 1.26 (br, 60H), 0.88 (br, 18H). ^{13}C-NMR (101 MHz, $CDCl_3$, δ): 157.81, 152.95, 140.68, 139.45, 138.81, 136.10, 129.22, 129.08, 128.27, 127.50, 125.34, 122.35, 120.31, 114.14, 108.49, 67.89, 64.81, 43.20, 38.79, 31.84, 31.80, 30.37, 29.75, 29.71, 29.37, 29.26, 27.28, 26.15, 26.10, 26.04, 22.68, 22.62, 14.12.

RESULTS AND DISCUSSION

Synthesis and Characterization

The synthesis of the grid-based nanomonomer and the polymerization are outlined in Scheme 2. In order to prepare the nanomonomer of polygrid, the grid nanomonomer with a rectangle shape can be synthesized by several possible routes starting from **L**-shape, **I**-shape or **U**-shape synthons. The molecular platform of fluorene-based nanogrids was established by us[34]. In fact, **L** shape synthon is the only method to obtain the grid-based nanomonomer with two bromide groups at diagonal position. Different from our previous reports, to make sure the solubility of the nanopolymers, 9-octyloxyphenylfluorenols rather than phenylfluorenols are introduced into the nanomonomer with octyl chain on the carbazole moiety. $BF_3{\cdot}Et_2O$-mediated Friedel-Crafts gridization is the effective way to close the electron-rich carbazole unit as the electrophilic arene with fluorenols[33, 35]. As a result, an **L**-shaped fluorenol is prepared firstly *via* a typical Suzuiki cross-coupling reaction between dibromide fluorine **1** and the key fluorenolboronic ester **2**. The monobromide **3** with the **L** shaped structure is effectively obtained with a yield of 86% by controlling the equivalent of 3:1 between compound **1** and **2**. After the Suzuki cross-coupling reaction, a gridization suffered from the dimerization of **L**-shape monomer under the condition of BFR with a yield of 24% for **NGM-Cz**. Consequently, the Yamamoto polymerization is smoothly carried out to prepare the one-dimensional polymergrid-based nanopolymer **PG-Cz**. Overall, the fluorene-based nanopolymer could be obtained concisely and smoothly *via* the Suzuki cross-coupling reaction, BFR and the Yamamoto polymerization. Both the nanomonomer of **NGM-Cz** and the nanopolymer of **PG-Cz** exhibit good solubility in common solvents such as chloroform, THF and toluene probably due to the long octyl and octoxy side chains of the substitutes at the 9-position of fluorenes, suggesting the fluorene-like building blocks have obvious advantage over other arenes or molecular segments.

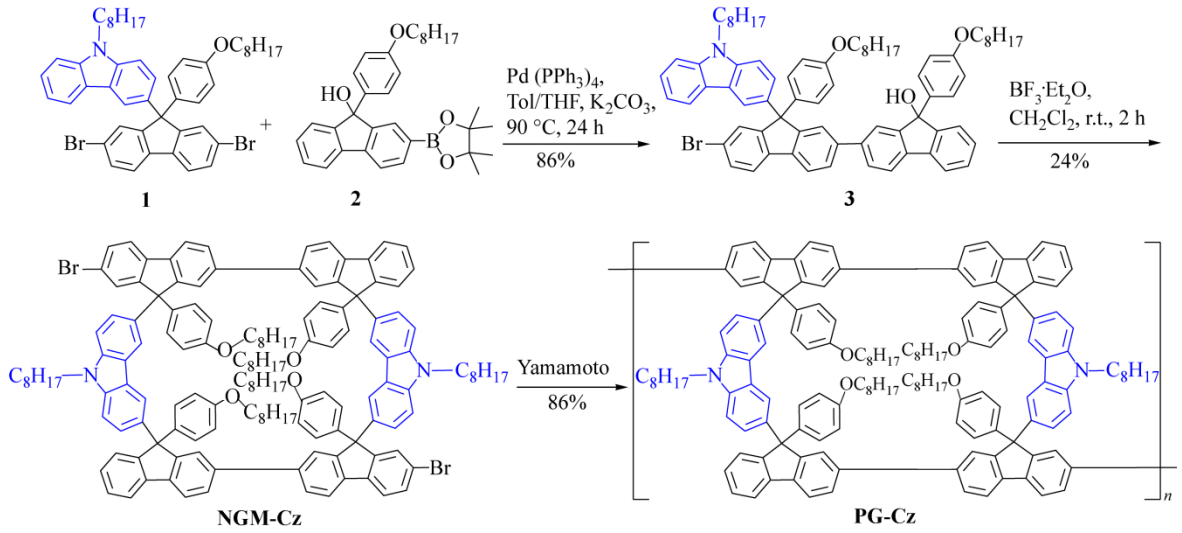

Scheme 2 The synthetic route of the grid nanomonomer and the grid-based nanopolymer

The purities and chemical structures of **NGM-Cz** and the nanopolymer **PG-Cz** are characterized by means of ^{1}H- and ^{13}C-NMR spectroscopy, MALDI-TOF-MS and others. Figures 1(a) and 1(b) show the ^{1}H-NMR spectra and ^{13}C-NMR spectra of **NGM-Cz** and its precursor 7'-bromo-9'-(9-octyl-9H-carbazol-3-yl)-9,9'-bis(4-(octyloxy)phenyl)-[2,2'-bifluoren]-9-ol, and the reference compound 2,7-dibromo-9-(4-(octyloxy)phenyl)-fluorene. It can be seen from the ^{1}H-NMR spectra of the precursor that the signal at δ = 2.46 is ascribed to the proton of hydroxyl group, and the chemical shift of about 3.9 is attributed to the proton at the α-carbon of alkoxy group. As can be seen in the ^{1}H-NMR spectrum of **NGM-Cz** (Fig. 1a), the proton of hydroxyl group at δ = 2.46 disappeared. In addition, the characteristic C-9 proton signal of 2,7-dibromo-9-(4-(octyloxy)phenyl)-fluorene around δ = 5.0 is not observed in **NGM-Cz**. These results illustrate that a cyclic compound is formed. Moreover, the proton signals around δ = 3.9 become broader, which is also ascribed to the hydrogen atom at the first methylene of alkoxy group in a more complicated chemical environment. With regard to the ^{13}C-NMR spectrum of **NGM-Cz**, the disappearance of the peak at δ = 83 suggests the disappearance of —OH group, indicating the effective transformation of C-9 of fluororenol in the precursor into C-9 of diarylfluorenes in **NGM-Cz**. The result from MALDI-TOF mass spectrometry supports the chemical structure of the grid nanomonomer **NGM-Cz**. It gives a peak with a molecular ion mass of m/z = 2185.7 that is consistent with a hydrocarbon of the molecular formula $C_{148}H_{156}Br_2N_2O_4$, which completely evident the cyclization (Fig. 1c). Furthermore, assignments are verified by carefully comparing the simulated isotopic distributions of the peaks with high-resolution experimental data. The simulated isotopic patterns for **NGM-Cz** shown in Fig. 1(d) perfectly match the experimental result. The grid-based nanopolymer is further characterized and confirmed by NMR spectra (Fig. S7) and gel permeation chromatography (GPC) (Fig. S1). GPC measurement reveals the molecular weight (M_n) of **PG-Cz** to be 1.04 × 10^4 Da (PDI = 1.6), indicating that the number of repeat units (n) is 5 for **PG-Cz**. It can be seen from Fig. 2(a) that **PG-Cz** exhibits outstanding thermal stability with a decomposition temperature (T_d) up to 342 °C (5% weight loss). However, no obvious glassy transition temperatures (T_g) were observed for **PG-Cz** (Fig. S2).

We further investigate the chain state of the nanopolymer in solution. Dynamic light scattering (DLS) was carried out at the condition of 0.5 mg/mL THF solution at room temperature, giving a root mean rectangular radius of gyration (R_g) of ~28.5 nm, the average hydrodynamic radius (R_h) of 10.2 nm and particle size distribution coefficient of 1.369, as a result, R_g/R_h = 28.5/10.2 ≈ 2.79 > 2.55. These data suggest the one-dimensional nanopolymer is the half-rigid chain in a single state without aggregates.

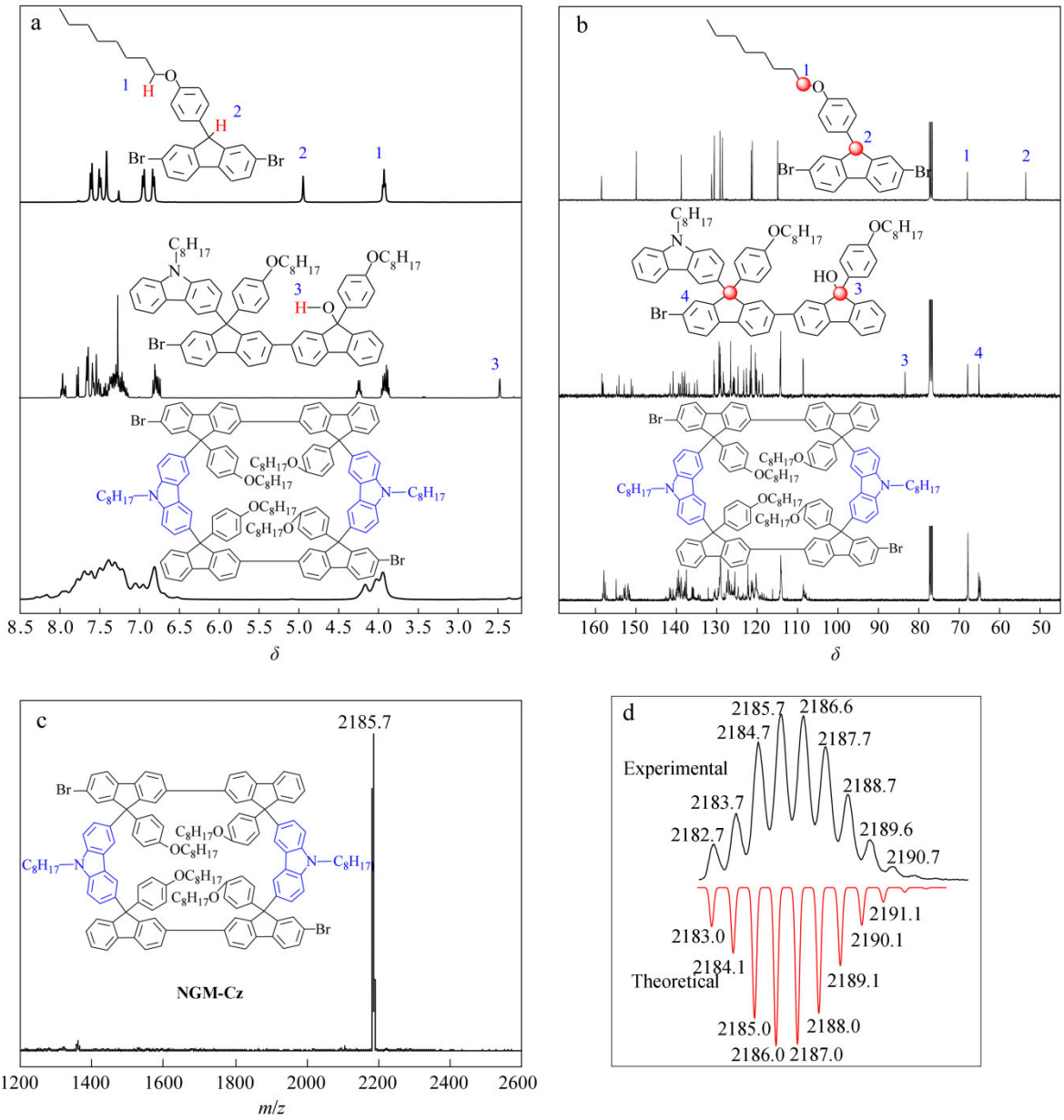

Fig. 1 (a) ^{1}H-NMR and (b) ^{13}C-NMR spectra of **NGM-Cz**, its precursor and the reference compounds; (c) MALDI-TOF mass spectrum of **NGM-Cz**; (d) comparison of experimental and theoretical MALDI-TOF mass spectra of **NGM-Cz**

Electrochemical Properties

Cyclic voltammetric (CV) measurement was carried out to investigate the electrochemical oxidation and reduction behaviors of **PG-Cz** and estimated the corresponding HOMO and LUMO energy levels. Figure 2(b) shows the CV curves of the nanopolymer **PG-Cz**. The oxidation onset potential is recorded at 0.86 V for **PG-Cz** versus Ag/Ag^{+}. As a result, the HOMO energy level is estimated to be −5.63 eV according to the empirical formula $E_{HOMO} = -(E_{ox} - E_{Fc}) - 4.8$ eV, where the value of E_{Fc} for ferrocene is 0.03 V versus Ag/Ag^{+}, and 4.8 eV is the energy level of ferrocene below vacuum. Probably, the HOMO value of **PG-Cz** is mainly attributed to the *N*-octylcarbazole moieties that are electron-rich groups and possess strong electron donating ability. Moreover, it is noteworthy that the HOMO value of polymer grid **PG-Cz** incorporating carbazole groups is in a good

agreement with that of PVK[38, 39]. It can be deduced that the first oxidation peak corresponds to the *N*-octylcarbazole group for **PG-Cz**. Similarly, the reduction onset potential is measured to be −2.47 V for the nanopolymer **PG-Cz**, from which the LUMO energy level of **PG-Cz** is calculated to be −2.30 eV. These results suggest that the nanopolymer **PG-Cz** has better electron-transporting ability than PVK owing to the introduction of fluorene groups.

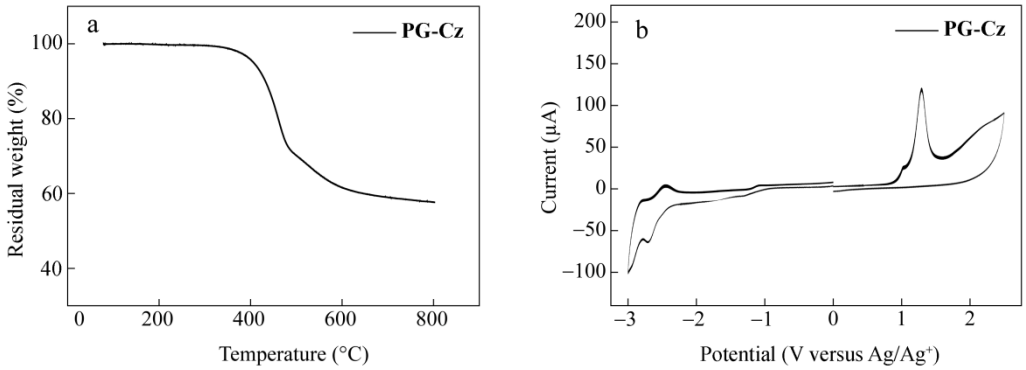

Fig. 2 (a) TGA curve and (b) cyclic voltammogram of the grid-based nanopolymer **PG-Cz**

Optical Properties

The electronic absorption spectra of the grid-based nanomonomer and the nanopolymer in toluene solutions are shown in Fig. 3. It can be seen from Fig. 3 that the nanogrid **NGM-Cz** displays the maximum absorption wavelength at 336 nm. Upon polymerization, a significant bathochromic shift of 23 nm (λ_{max} = 359 nm) can be observed, due to the extended π-conjugation of tetrafluorene. In the case of tetrafluorene, the absorption maximum is around 367 nm[15], which shows a little more bathochromic than the nanopolymer probably due to the change of conformation. Additionally, compared to polyfluorene ($\lambda_{max} \approx$ 390 nm), the polymer grid shows a hypsochromic shift in the wavelength of maximum absorption owing to the conjugation-interrupted feature with tetrafluorene units[14, 17].

Furthermore, the solvatochromic effects on the absorption and PL features of **PG-Cz** are also investigated in the polar and nonpolar solvents (Fig. 3b). As illustrated in Fig. 3(b), no obvious shifts of maximum absorption and maximum emission are observed for **PG-Cz** in these solvents, indicating the obtained nanopolymer is suitable for solution processing. To study the intermolecular interactions of this polygrid, the absorption spectra of **PG-Cz** with different concentrations were recorded. The result is displayed in Fig. 3(c). With the concentration increasing from 0.001 mg/mL to 0.1 mg/mL, no obvious shift of the maximum wavelength can be observed. The result indicates that very weak intermolecular interactions exist in the nanopolymer, which is ascribed to the large steric hindrance of the nanogrid monomer containing four diarylfluorene moieties with four sp^3 carbon atoms. The low solvent dependence and weak intermolecular interactions of the grid-based nanopolymer are of great significance to prepare uniform thin films and thus obtain high-efficiency photoelectronic devices from the corresponding nanoink. Moreover, we also investigated the effect of different concentrations of nanoink on the UV-Vis and PL spectra. As demonstrated in Fig. 3(d), no obvious change is observed, which is quite important for the solution processing. In addition, thermal annealing at 180 °C in air and under N_2 were further conducted to study the spectral stability for the nanopolymer films (Figs. 3e and 3f). It can be seen from Figs. 3(e) and 3(f) that there is almost no change in the UV-Vis spectra of **PG-Cz** films after annealing in air or under N_2 for 10 h. With regard to fluorescence emission spectra, a slight increase in the low-energy green band at the center of 500–600 nm was observed after thermal annealing in air for 10 h, and this green emission is probably ascribed to the emissive fluorenone defects owing to the thermo-oxidative degradation of the polyfluorene backbone[40]. While there is no difference after annealing under N_2, illustrating that the grid-based nanopolymer **PG-Cz** has relatively good thermal stability. Moreover, time-resolved

photoluminescence spectrum (Fig. S3) shows that the films of nanopolymer **PG-Cz** possess a long fluorescent longevity of 865 ps. Impressively, the nanopolymer solution exhibits a longer fluorescent longevity of up to 2626 ps, which is over 3 times than that of the film. The PL quantum yields (Φ_{PLQY}) in solution and in film are ~82% and ~31% for **PG-Cz**, respectively. Importantly, for the **PG-Cz** film, the high thermal stability, good PL quantum yield and longer fluorescent longevity indicate its better potential for the photoelectronic applications, such as the polymer light emitting diode and lasers.

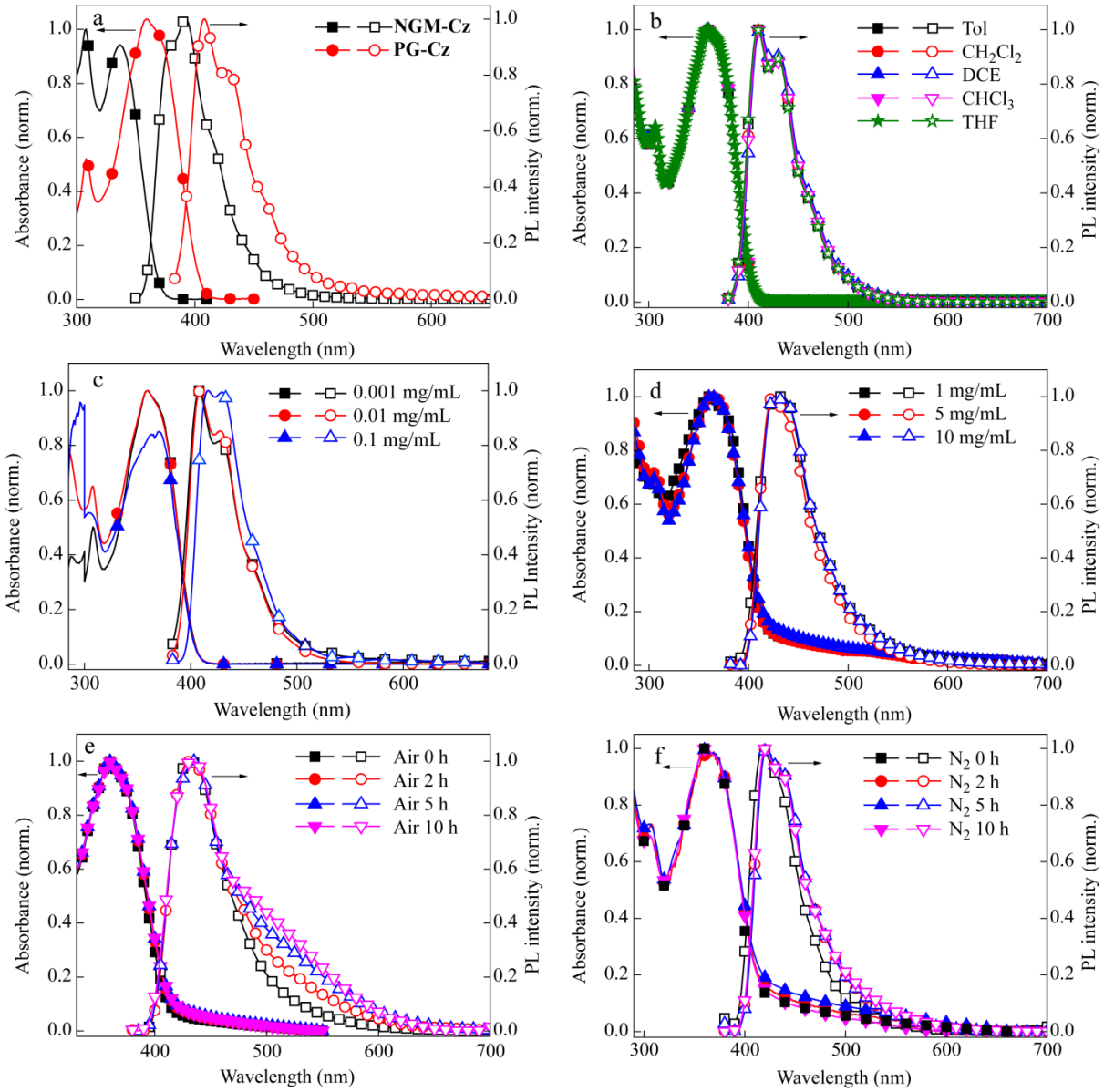

Fig. 3 UV-Vis and PL spectra of the nanogrid monomers and the polymer grids in various states: (a) nanogrid monomers (10^{-5} mol/L) and polymer grids (0.01 mg/mL) in dilute toluene solution; (b) **PG-Cz** in different solvents; (c) **PG-Cz** in toluene solutions with different concentrations; (d) **PG-Cz** thin films from toluene solutions with different concentrations; (e) **PG-Cz** films from toluene solution (10 mg/mL) after thermal annealing at 180 °C in air for 0, 2, 5 and 10 h; (f) **PG-Cz** films from toluene solution (10 mg/mL) after thermal annealing at 180 °C under N_2 for 0, 2, 5 and 10 h

CONCLUSIONS

In conclusion, we have proposed organic nanomonomers for optoelectronic nanopolymers that are different from the inorganic counterparts. We have synthesized a soluble nanopolymer with the excellent stabilities from the nanomonomers. The nanopolymer consists of fluorene-based nanogrids as the repeat units. This nanogrid monomer has a rectangular shape of ~1.7 nm × 1.2 nm with difluorene as the arms and carbozale moiety as the rungs. Owing to precursor substituents that could suffer the Friedel-Craft gridization in the acid condition, the nanogrid monomers were easily obtained by cyclization. The soluble nanopolymer with the advantages of both polymers and nano-objects offers the possibility of multiple functions integrated into a nanoscale one-dimensional polymer chain, which may become the starting point of the next generation of polymeric materials after semiconducting and metallic polymers[41].

REFERENCES

1 Balzani, V., Bergamini, G. and Ceroni, P., Angew. Chem. Int. Ed., 2015, 54: 11320
2 Pust, P., Schmidt, P.J. and Schnick, W., Nat. Mater., 2015, 14: 454
3 Lin, Z.Q., Liang, J., Sun, P.J., Liu, F., Tay, Y.Y., Yi, M.D., Peng, K., Xia, X.H., Xie, L.H., Zhou, X.H., Zhao, J.F. and Huang, W., Adv. Mater., 2013, 25: 3664
4 Möller, S., Perlov, C., Jackson, W., Taussig, C. and Forrest, S.R., Nature, 2003, 426: 166
5 Xie, L.H., Yin, C.R., Lai, W.Y., Fan, Q.L. and Huang, W., Prog. Polym. Sci., 2012, 37: 1192
6 Heremans, P., Gelinck, G.H., Muller, R., Baeg, K.J., Kim, D.Y. and Noh, Y.Y., Chem. Mater., 2010, 23: 341
7 Kulkarni, A.P., Tonzola, C.J., Babel, A. and Jenekhe, S.A., Chem. Mater., 2004, 16: 4556
8 Uoyama, H., Goushi, K., Shizu, K., Nomura, H. and Adachi, C., Nature, 2012, 492: 234
9 Chen, J. and Cao, Y., Acc. Chem. Res., 2009, 42: 1709
10 Wu, W., Liu, Y. and Zhu, D., Chem. Soc. Rev., 2010, 39: 1489
11 Chi, C., Im, C., Enkelmann, V., Ziegler, A., Lieser, G. and Wegner, G., Chem. Eur. J., 2005, 11: 6833
12 List, E.J., Guentner, R., Scanducci de Freitas, P. and Scherf, U., Adv. Mater., 2002, 14: 374
13 Lin, J., Yu, Z., Zhu, W., Xing, G., Lin, Z., Yang, S., Xie, L., Niu, C. and Huang, W., Polym. Chem., 2013, 4: 477
14 Lin, J.Y., Zhu, W.S., Liu, F., Xie, L.H., Zhang, L., Xia, R., Xing, G.C. and Huang, W., Macromolecules, 2014, 47: 1001
15 Liu, Y.Y., Lin, J.Y., Bo, Y.F., Xie, L.H., Yi, M.D., Zhang, X.W., Zhang, H.M., Loh, T.P. and Huang, W., Org. Lett., 2016, 18: 172
16 Xie, L.H., Ling, Q.D., Hou, X.Y. and Huang, W., J. Am. Chem. Soc., 2008, 130: 2120
17 Lin, Z.Q., Shi, N.E., Li, Y.B., Qiu, D., Zhang, L., Lin, J.Y., Zhao, J.F., Wang, C., Xie, L.H. and Huang, W., J. Phys. Chem. C, 2011, 115: 4418
18 Zhao, Z., Chan, C.Y., Chen, S., Deng, C., Lam, J.W., Jim, C.K., Hong, Y., Lu, P., Chang, Z. and Chen, X., J. Mater. Chem., 2012, 22: 4527
19 Lei, T., Wang, J.Y. and Pei, J., Chem. Mater., 2013, 26: 594
20 Kang, I., Yun, H.J., Chung, D.S., Kwon, S.K. and Kim, Y.H., J. Am. Chem. Soc., 2013, 135: 14896
21 Mei, J. and Bao, Z., Chem. Mater., 2013, 26: 604
22 Wang, Y., Liu, Y., Chen, S., Peng, R. and Ge, Z., Chem. Mater., 2013, 25: 3196
23 Jiang, Y.R., Zhang, H.X., Zhang, K.X. and Zhang, Q.Y., Chinese J. Polym. Sci., 2015, 33: 490
24 Harada, A., Takashima, Y. and Nakahata, M., Acc. Chem. Res., 2014, 47: 2128
25 Brovelli, S., Sforazzini, G., Serri, M., Winroth, G., Suzuki, K., Meinardi, F., Anderson, H.L. and Cacialli, F., Adv. Funct. Mater., 2012, 22: 4284
26 Wei, P., Yan, X. and Huang, F., Chem. Soc. Rev., 2015, 44: 815
27 Chang, C.Y., Cheng, Y.J., Hung, S.H., Wu, J.S., Kao, W.S., Lee, C.H. and Hsu, C.S., Adv. Mater., 2012, 24: 549
28 Kaltenbrunner, M., Sekitani, T., Reeder, J., Yokota, T., Kuribara, K., Tokuhara, T., Drack, M., Schwödiauer, R., Graz, I.

and Bauer-Gogonea, S., Nature, 2013, 499: 458
29 Jiang, Z., Ye, T., Yang, C., Yang, D., Zhu, M., Zhong, C., Qin, J. and Ma, D., Chem. Mater., 2010, 23: 771
30 Liu, B., Lin, J., Lei, Z., Sun, M., Xie, L., Xue, W., Yin, C., Zhang, X. and Huang, W., Macromol. Chem. Phys., 2015, 216: 1043
31 Yin, C.R., Han, Y., Li, L., Ye, S.H., Mao, W.W., Yi, M.D., Ling, H.F., Xie, L.H., Zhang, G.W. and Huang, W., Polym. Chem., 2013, 4: 2540
32 Wei, F., Li, H., Song, C., Ma, Y., Zhou, L., Tung, C.H. and Xu, Z., Org. Lett., 2015, 17: 2860
33 Zhang, G., Wei, Y., Wang, J., Liu, Y., Xie, L., Wang, L., Ren, B. and Huang, W., Mater. Chem. Front., 2017, DOI: 10.1039/C6QM00004E
34 Wang, L., Zhang, G.W., Ou, C.J., Xie, L.H., Lin, J.Y., Liu, Y.Y. and Huang, W., Org. Lett., 2014, 16: 1748
35 Lin, J., Li, W., Yu, Z., Yi, M., Ling, H., Xie, L., Li, S. and Huang, W., J. Mater. Chem. C, 2014, 2: 3738
36 Liu, Z.D., Chang, Y.Z., Ou, C.J., Lin, J.Y., Xie, L.H., Yin, C.R., Yi, M.D., Qian, Y., Shi, N.E. and Huang, W., Polym. Chem., 2011, 2: 2179
37 Chang, Y.Z., Shao, Q., Bai, L.Y., Ou, C.J., Lin, J.Y., Xie, L.H., Liu, Z.D., Chen, X., Zhang, G.W. and Huang, W., Small, 2013, 9: 3218
38 Yin, C.R., Ye, S.H., Zhao, J., Yi, M.D., Xie, L.H., Lin, Z.Q., Chang, Y.Z., Liu, F., Xu, H., Shi, N.E., Qian, Y. and Huang, W., Macromolecules, 2011, 44: 4589
39 Li, L., Hu, T.Q., Yin, C.R., Xie, L.H., Yang, Y., Wang, C., Lin, J.Y., Yi, M.D., Ye, S.H. and Huang, W., Polym. Chem., 2015, 6: 983
40 Gong, X., Iyer, P.K., Moses, D., Bazan, G.C., Heeger, A.J. and Xiao, S.S., Adv. Funct. Mater., 2003, 13: 325
41 Xie, L.H. and Huang, W. “Supramolecular steric hindrance at bulky organic/polymer semiconductors and devices, in non-covalent interactions in the synthesis and design of new compounds”, ed. by Maharramov, A.M., Mahmudov, K.T., Kopylovich, M.N. and Pombeiro, A.J.L., John Wiley & Sons, Inc, Hoboken New Jersey, 2016, p. 443